



Published in final edited form as:

Photochem Photobiol. 2013 ; 89(5): 1199–1207. doi:10.1111/php.12104.

Protective Effect of Tropical Highland Blackberry Juice (*Rubus adenotrichos* Schldl.) Against UVB-Mediated Damage in Human Epidermal Keratinocytes and in a Reconstituted Skin Equivalent Model

Laura Calvo-Castro^{1,2}, Deeba N. Syed³, Jean C. Chamcheu³, Fernanda M. P. Vilela⁴, Ana M. Pérez⁵, Fabrice Vaillant⁵, Miguel Rojas^{1,†}, and Hasan Mukhtar^{3,*†}

¹Centro de Investigación en Biotecnología, Instituto Tecnológico de Costa Rica, Cartago, Costa Rica

²Centro de Investigación en Estructuras Microscópicas, Universidad de Costa Rica, San José, Costa Rica

³Department of Dermatology, University of Wisconsin, Madison, WI

⁴Faculty of Pharmaceutical Sciences of Ribeirao Preto, University of Sao Paulo, Ribeirao Preto, Brazil

⁵Centro Nacional de Ciencia y Tecnología de los Alimentos, Universidad de Costa Rica, San José, Costa Rica

Abstract

Solar ultraviolet (UV) radiation, particularly its UVB (280–320 nm) spectrum, is the primary environmental stimulus leading to skin carcinogenesis. Several botanical species with antioxidant properties have shown photochemopreventive effects against UVB damage. Costa Rica's tropical highland blackberry (*Rubus adenotrichos*) contains important levels of phenolic compounds, mainly ellagitannins and anthocyanins, with strong antioxidant properties. In this study, we examined the photochemopreventive effect of *R. adenotrichos* blackberry juice (BBJ) on UVB-mediated responses in human epidermal keratinocytes and in a three-dimensional (3D) reconstituted normal human skin equivalent (SE). Pretreatment (2 h) and posttreatment (24 h) of normal human epidermal keratinocytes (NHEKs) with BBJ reduced UVB (25 mJ cm⁻²)-mediated (1) cyclobutane pyrimidine dimers (CPDs) and (2) 8-oxo-7,8-dihydro-2'-deoxyguanosine (8-oxodG) formation. Furthermore, treatment of NHEKs with BBJ increased UVB-mediated (1) poly(ADP-ribose) polymerase cleavage and (2) activation of caspases 3, 8 and 9. Thus, BBJ seems to alleviate UVB-induced effects by reducing DNA damage and increasing apoptosis of damaged cells. To establish the *in vivo* significance of these findings to human skin, immunohistochemistry studies were performed in a 3D SE model, where BBJ was also found to decrease CPDs formation. These data suggest that BBJ may be developed as an agent to ameliorate UV-induced skin damage.

INTRODUCTION

There is considerable evidence showing that solar ultraviolet (UV) radiation, particularly its UVB (280–320 nm) component, is the main agent responsible for both the initiation and progression phases of all types of skin cancer (1–3), a phenomenon now referred to as photocarcinogenesis (4,5). Nonmelanoma skin cancers, involving both basal cell and squamous cell carcinomas (1), are the most frequent (although rarely fatal) form of cancer in light-skinned populations (2,6). In contrast, melanoma is a relatively low-incidence type of cancer, but it is highly invasive and incurable in most metastatic patients, highlighting the importance of its prevention and treatment in early stages (7). Even though public health initiatives have increasingly promoted sun protection awareness around the globe, the worldwide incidence of skin cancer continues to rise at an alarming rate (2,7).

Increasing evidence supports chemoprevention approaches based on diverse botanical agents as an alternative for ameliorating the carcinogenesis process in the skin (3,4,7,8). Dietary polyphenols predominate among the most common phytochemical agents for which anti-carcinogenic, including photochemopreventive properties, have been described (4,5,7). These botanical agents exhibit antioxidant, anti-inflammatory, anti-proliferative and DNA repair properties with potential photoprotective and/or photochemopreventive applications (1,5).

In this regard, the potential anticancer properties of berry fruits have been described (9–11). Berries are highly concentrated in a vast amount of phytochemicals, most of which are phenolic compounds, including flavonoids, condensed and hydrolyzable tannins, stillbenoids, phenolic acids, lignans, triterpenes and sterols. *In vitro* and *in vivo* studies have shown that these berry phenolics possess strong antioxidant and anti-inflammatory properties, as well as several other anti-carcinogenic-related activities that have been thoroughly reviewed elsewhere (9,12). Given that cumulative oxidatively generated damage to DNA seems to be significant in cancer development, many chemoprevention studies have focused on botanical agents with relevant antioxidant properties (11).

Blackberries (*Rubus* sp.) rank highly among fruits with strong antioxidant activities (13,14). Tropical highland blackberry (*Rubus adenotrichos* Schldl.), also part of Andean blackberries (15), contains appreciable levels of phenolic compounds, mainly ellagitannins and anthocyanins (16,17), two of the most common phenolic compounds in berries that have been related to antioxidant activity in these fruits (12). Previous studies (16,18) have shown that even though *R. adenotrichos* has a relatively low anthocyanin content (when compared with other temperate climate cultivars), it also has the highest content of ellagitannins ever reported in any other edible fruit, exhibiting a relatively high antioxidant capacity.

In this study, we investigated the effect of treating normal human epidermal keratinocytes (NHEKs) and a three-dimensional (3D) model of reconstituted normal human skin equivalent (SE), with Costa Rica's tropical highland blackberry juice (BBJ), before and after exposure to UVB radiation (25 mJ cm⁻²). We show that BBJ reduced UVB-mediated DNA damage with concomitant increase in the apoptotic response of the UVB-damaged cells, suggesting a potential chemopreventive effect.

MATERIALS AND METHODS

Antibodies and reagents

Cyclobutane pyrimidine dimers (CPD; MC-062) and 8-oxo-7,8-dihydro-2'-deoxyguanosine (8-oxodG, sc-139586) primary antibodies were obtained from Kamiya Biomedical Company (Seattle, WA) and Santa Cruz Biotechnology (Dallas, TX) respectively. Primary antibodies

for p53 (#9282), phospho-p53 (p-p53; #9284) (Ser15), poly (ADP-ribose) polymerase (PARP; #9542), caspase 3 (#9662), cleaved caspase 8 (Asp391; #9496), caspase 9 (#9502) and anti-mouse (#7074) or anti-rabbit (#7076) secondary antibody horse radish peroxidase (HRP) conjugates were purchased from Cell Signaling Technology (Beverly, MA). The BCA™ protein assay kit and SuperSignal^R West Pico chemiluminescent substrate kit were purchased from Pierce (Thermo Scientific, Rockford, IL). The mini-protean precast Tris-Glycine gels were from BioRad (Hercules, CA). Anti-mouse or anti-rabbit secondary antibody biotinylated HRP conjugates for immunohistochemistry (IHC) or immunocytochemistry (ICC) were obtained from Vector Laboratories (Burlingame, CA). Annexin-V-FLUOS staining kit was purchased from Roche Diagnostic Corporation (Indianapolis, IN).

Clarified BBJ

Frozen (−20°C) mature fruits of Costa Rica's tropical highland blackberry (*Rubus adenotrichos* cv *Vino con espinas*) were purchased from a grower's cooperative (APROCAM, Cartago, Costa Rica). Blackberries were thawed for 24 h in a 5°C chamber and then pressed (300 kPa for 5 min; Hydraulic Shop Press OTC 25 Ton, Owatonna, USA) and macerated with a commercial enzymatic preparation (Klerzyme[®] 150 from DSM Food Specialties, Heerlen, the Netherlands) for 1 h at 35°C under constant agitation. The juice obtained was clarified by cross-flow microfiltration, performed as described previously (19), in a pilot-scale microfiltration unit at (35 ± 1)°C, 150 kPa trans-membrane pressure and 5 m s^{−1} cross-flow velocity until reaching a volume reduction ratio (VRR) of 10. The clarified microfiltered juice (MFT BBJ) obtained was then packed in high-density polyethylene bags and kept at −20°C until use.

To obtain a juice with increased concentration in ellagitannins (specifically Lambertianin C and Sanguin H5, with respective average molecular weight of 2805.81 and 1871.27 g mole^{−1}), MFT BBJ was treated by cross-flow ultrafiltration (CFU) using a pilot unit (Iberlact, Spain) equipped with a flat-sheet tight ultrafiltration membrane with a molecular weight cut-off of 1 kDa (GK, GE Osmonics, USA) with an effective membrane area of 0.0139 m². CFU was performed at 30°C, 2 MPa of transmembrane pressure and 0.93 m s^{−1} cross-flow velocity until reaching a VRR of 1.8. The retentate obtained from CFU (so on referred to as the ultrafiltered juice [UFT BBJ]) was then packed in high-density polyethylene bags and kept at −20°C until use.

Moisture and total titratable acidity (expressed as malic acid equivalents) were determined using standard AOAC methods 920.151 and 942.15 (20) respectively. Total soluble solids (expressed as °Brix) were measured as described previously (16) on a digital refractometer with automatic temperature compensation ("Pallete" PR-100; Atago Co. Ltd., Tokyo, Japan). Analyses of total anthocyanins (expressed as cyanidin-3-glucoside [Cy-3-glc] equivalents) and ellagitannins (expressed as ellagic acid equivalents) were done by HPLC/DAD using the same system, column, conditions, standards and solvents as described by Mertz *et al.* (17), with the following changes: solvent flow rate was set at 0.3 mL min^{−1}, gradient conditions were from 5% to 25% solvent B (2% aqueous formic acid) in 20 min, from 25% to 100% solvent B in 5 min, from 100% to 10% solvent B in 5 min and from 10% to 5% solvent B in 5 min.

Cell isolation and culture

Immortalized human keratinocytes (HaCaT) and Swiss albino 3T3 fibroblasts (CCL-92, ATCC) were both maintained in DMEM medium (4.5 g L^{−1} glucose; GIBCO, Invitrogen) supplemented with 10% FBS (GIBCO), 2% L-glutamine (4 mM; GIBCO), 1% sodium pyruvate (0.11 mg mL^{−1}; Sigma) and 1% antibiotics (10 000 IU mL^{−1} penicillin and 10 000

$\mu\text{g mL}^{-1}$ streptomycin; GIBCO). NHEKs and normal human dermal fibroblasts (NHDFs) cultures were established as described (21,22). Submerged NHEKs cultures were maintained in serum-free Epi-Life growth medium supplemented with Human Keratinocytes Growth Supplement (Cascade Biologics Inc, Portland, OR) and 3D cultures were grown in the medium as described below. NHDFs were grown in DMEM medium (CellGro, Mediatech Inc., Manassas, VA) supplemented with 10% FBS (CellGro) and 1% antibiotics–antimycotics ($10\,000\text{ IU mL}^{-1}$ penicillin, $10\,000\ \mu\text{g mL}^{-1}$ streptomycin and $25\ \mu\text{g mL}^{-1}$ amphotericin; CellGro). All cells were maintained at 95% humidity in 5% CO_2 environment at 37°C . NHEKs and NHDFs between passages 2–9 were used in this study.

Generation of 3D full-thickness SEs

Full-thickness SE model was generated as described previously (21,22), with slight modifications using NHEKs and NHDFs (passages 2–4). Cultures were maintained at air-liquid interphase for 11 days to reconstitute a 3D multilayered SE consisting of a dermal substratum and an outermost differentiating epidermis.

For the dermal component was first prepared a noncellular layer mainly composed of equilibrated collagen, followed by a cellular layer consisting of fibroblasts (5×10^5 cells mL^{-1}) embedded in a collagen matrix (1 part $10\times$ DMEM, 8 parts rat tail collagen type I and 1 part mixture of L-glutamine, FBS and 7.5% sodium bicarbonate; pH 7.4). From this mixture, 250 μL was poured into each well of 0.4 μm pore size Millicell-PCF inserts (12 mm diameter; Millipore Corporation, Billerica, MA), each placed in wells of a six-well plate, and then equilibrated for gelation for an hour. The inserts containing the dermal layer were incubated for 2 days fully immersed in DMEM medium containing 5% FBS and 1% antibiotics–antimycotics, until gel contraction was observed. Before adding the epidermal layer, dermal tissue was washed with $1\times$ PBS and incubated in Progenitor Cell Targeted Culture Media (CnT-02-07, CellnTec; Zen-Bio Inc., Research Triangle Park, NC) for 1 h at 37°C .

For epidermal layers, second-to-fourth passage NHEKs at 30% confluence were synchronically switched to and maintained in CnT-02-07 prior to harvest and generation of 3D SE cultures. After trypsinization, 1.2×10^6 keratinocytes were seeded on top of the dermal layer in each insert and incubated for 3 days completely immersed in CnT-02-07, followed by immersed incubation in differentiation medium (CnT-02-3DP5; CellnTec, Zen-Bio Inc.) for another 2 days. The reconstructed tissue composite was then lifted to the air-liquid interface (ALI) by placing the inserts on a custom cell culture stand (MatTek Corporation, Ashland, MA) and only replenishing the medium outside the insert with 4 mL of CnT-02-3DP5. Composites were maintained at the ALI until treatment and harvest. Both CnT-02-07 and CnT-02-3DP5 were supplemented with 1% antibiotics–antimycotics solution, and media were changed every alternate day.

When harvested, tissue was fixed in 10% neutral-buffered formalin for further analysis. For immunochemistry, one sample of each treatment was stained with hematoxylin and eosin (H&E) to check cellular and tissue structures.

Cell viability assay

The effect of BBJ on the viability of cells was determined by MTT assay and phase contrast microscopy as described previously (23). Briefly, cells (70–80% confluent) were treated for 24 h in 24-well plates with MFT or UFT diluted 1:5, 1:10, 1:50, 1:100, 1:150, 1:300 and 1:500 in the respective culture medium for each cell line, after which the medium was removed and cells were washed with PBS and incubated for 2 h in MTT reagent (300 μL , $0.5\ \text{mg mL}^{-1}$ final concentration in medium). The MTT solution was removed and the

formazan crystals were dissolved in DMSO (300 μ L), and absorbance was recorded at 540 nm on a Multiscan MCC/340 microplate reader (ThermoLabsystems, Fisher). Treatment with each MFT or UFT dilution was repeated in three wells in three independent experiments. The effect of UVB (25 mJ cm^{-2}) on the viability of NHEKs was determined 24 h after UVB exposure using the same procedure.

Exposure of cells and SEs to UVB

Normal human epidermal keratinocytes (70–80% confluent) and SEs were irradiated in PBS with UVB (25 mJ cm^{-2}) using a custom designed Research Irradiation Unit (Daavlin, Bryan, OH) as described previously (24). Twenty-four hours post-UVB exposure, cells were harvested for cell viability determination or ICC, or cell lysates were prepared. SEs were harvested for IHC.

Pre- and posttreatment of cells and SEs with BBJ

In the pretreatment, NHEKs (70–80% confluent) were incubated for 2 h with UFT BBJ diluted 1:300 and 1:500 in Epi-Life medium. Then, cells were washed with PBS and irradiated with UVB (25 mJ cm^{-2}) while fully submerged in fresh PBS. Twenty-four hours post-UVB exposure, cells were harvested for immunochimistry or immunoblotting. In the posttreatment, NHEKs were first irradiated with UVB (25 mJ cm^{-2}) and then treated with the same UFT dilutions (1:300 or 1:500) for 24 h. Cells were then washed with PBS and immediately harvested. SEs were pre- (2 h) and post (24 h) treated with UFT BBJ diluted in CnT-02-3DP5 medium. Here, UFT BBJ was applied both topically, by directly pouring a 10 μ L droplet of UFT solution on top of the tissue, and in growth medium underneath by adding 4 mL of the UFT solution outside the insert. For UVB irradiation (25 mJ cm^{-2}), SEs were washed and kept in PBS at the ALI. Upon harvest, tissues were fixed in 10% neutral-buffered formalin, embedded in paraffin and processed as described below.

Preparation of total cell lysates

Cells treated with UVB and/or BBJ (UFT) were washed twice with PBS and incubated for 15 min with 0.15 mL ice-cold RIPA lysis buffer (25 mM Tris-HCl pH 7.6, 150 mM NaCl, 1% NP-40, 1% sodium deoxycholate, 0.1% SDS; Pierce Biotechnology, Rockford, IL) with freshly added protease inhibitor cocktail (Protease Inhibitor Cocktail Set III; Calbiochem, La Jolla, CA) and 0.2 mM sodium vanadate. Homogenized lysates were then centrifuged at 15 294 g for 25 min at 4°C to remove cell debris and the supernatant (total cell lysate) was collected and stored at -80°C. The protein concentration was determined by BCA protein assay kit according to the manufacturer's protocol.

Western blot analysis

For western blotting, 25–40 μ g protein was electrophoresed on 12% polyacrylamide gels and transferred to a nitrocellulose membrane. The blot was blocked in blocking buffer (7% nonfat dry milk, 1% Tween 20; in 20 mM Tris-buffered saline, pH 7.6) for 1 h at room temperature and incubated with appropriate primary antibody in blocking buffer for 2 h to overnight at 4°C, followed by 2 h incubation at room temperature with anti-mouse or anti-rabbit secondary HRP-conjugated antibody. The membrane was washed and bound complex detected by chemiluminescence (ECL kit; Amersham Biosciences, UK) and autoradiography using XAR-5 film (Eastman Kodak Co., Rochester, NY) or developed by digital camera using the program ChemiDoc XRS Software (BioRad).

Apoptosis detection by fluorescent microscopy

Apoptotic cells were detected with the Annexin-V-FLUOS staining kit according to the manufacturer's protocol. Briefly, cells were stained with annexin V (green fluorescence) and

the fluorescence was visualized using a Nikon Eclipse Ti system (Nikon Instruments Inc., Tokyo, Japan). Digital images were captured with an attached CoolSNAP camera (Roper Scientific, Trenton, NJ) linked to a computer.

Immunocytochemistry

For immunocytochemical analysis, NHEKs were seeded in 8-well tissue culture slides (70–80% confluent) and treated with UVB and/or UFT BBJ. Twenty-four hours after treatment, cells were washed with PBS and fixed in 4% paraformaldehyde in PBS for 30 min to overnight at 4°C, followed by three washes with PBS and three quick washes with 0.25% Triton-X. Cells were incubated for 20 min with 3% H₂O₂ in methanol, washed thrice with PBS and incubated for 15 min with Background Sniper (Biocare Medica, Concord, CA), followed by overnight incubation at 4°C with CPD or 8-oxodG primary antibodies (1:200 and 1:50, respectively, in 2% bovine serum albumin, 5% normal goat serum [NGS] and 0.2% Triton-X in PBS). Then, cells were washed once with PBS and incubated with biotinylated HRP-conjugated secondary antibodies (1:500 in the same dilution buffer) for 2 h at room temperature in the dark, followed by treatment with ABC Conjugate (R.T.U. Vectastain[®] Kit, Burlingame, CA) for 30 min and incubation with 3,30-diaminodenzidine (Dako Corp., CA) until desired stain intensity developed. Cells were counterstained with 10% hematoxylin (Vector) in water, dehydrated through graded ethanol series, cleared in xylene and mounted in xylene-based mounting medium. Staining was visualized using a Nikon Eclipse Ti inverted microscope as described before.

Immunohistochemistry

Immunohistochemical analysis was performed as described by Khan *et al.* (1) with a few modifications. The reconstituted human SE was harvested 24 h after treatment with UVB and/or UFT. Formalin-fixed and paraffin-embedded 5 µm cryo-sections were deparaffinized in xylene, rehydrated through an ethanol gradient (100–50%) and washed with water. For antigen retrieval, sections were incubated in 10 mM citrate buffer (pH 6.0) for 10 min at 95°C and then immediately cooled down to room temperature for 30 min, followed by three washes with water. Endogenous peroxidase was quenched by incubation in 0.3% hydrogen peroxide for 30 min, and washed thrice with washing buffer (0.2% Triton-X in PBS). Nonspecific binding sites were blocked by incubation with 2.5% NGS in blocking buffer for 20 min, followed by overnight incubation (4°C) with primary antibody against CPD and 8-oxodG (1:200 and 1:50, respectively, in blocking buffer). Cells were washed with PBS and incubated with biotinylated HRP-conjugated secondary antibodies (1:500 in the same dilution buffer), followed by treatment with ABC Conjugate (R.T.U. Vectastain[®] Kit) and incubation with 3,30-diaminodenzidine (Dako Corp) as described above for ICC. Tissue sections were counterstained with 10% hematoxylin (Vector), and processed for visualization as described above.

Antioxidant activity

The antioxidant capacity of UFT BBJ (1:300 and 1:500 dilutions) in NHEK cell lysates was determined as described earlier (23) using a trolox antioxidant assay kit (Cayman Chemical, Ann Arbor, MI), following the manufacturer's protocol. The assay compares the ability of the antioxidants in a cell lysate to inhibit the oxidation of ABTS^R (2,2'-azino-di-[3-ethylbenzthiazoline sulfonate]) to ABTS^{R•+} by metmyoglobin, against that of trolox, a water-soluble tocopherol analogue (23).

Statistical analysis

Results were expressed as the means \pm SD. Statistical analysis between controls and treatments were performed by Student's *t*-test, where a $P < 0.05$ was considered statistically significant.

RESULTS AND DISCUSSION

Physicochemical analysis

Moisture, pH and total titratable acidity were similar in both BBJ preparations (MFT and UFT). However, soluble solids and ellagitannins and anthocyanins content were higher in the UFT (Table 1). Soluble solids content of MFT was consistent with the literature (19) and, for both juice preparations, it was close to that reported for the water solubilized pulp of *R. adenotrichos* fruit (17) and other blackberry cultivars (25). Furthermore, pH and acidity in both juice preparations corresponded well to the reported values for *R. adenotrichos* water solubilized fruit (16,17). As expected (15–17,26), both juice preparations presented an ellagitannins content much higher than that of anthocyanins.

UFT BBJ did not protect NHEKs against UVB-mediated decrease in cell viability and total cellular oxidation induced by UVB

First, to establish a noncytotoxic BBJ treatment, we evaluated the effect of seven dilutions (1:5, 1:10, 1:50, 1:100, 1:150, 1:300 and 1:500) of both BBJ preparations (MFT and UFT) on the viability of two fibroblast cell lines (3T3 and NHDFs) and two keratinocyte cell lines (HaCaT and NHEKs). For further experimentation, we chose the 1:300 and 1:500 dilutions of the UFT BBJ, which showed no significant decrease ($P < 0.05$) in NHEKs cell viability to that of the untreated control (Fig. 1). Normal keratinocytes and the reconstituted SE treated with such UFT dilutions presented no morphological evidence of cytotoxicity either (Figs. 2b and 5a); nevertheless, a slightly different cell morphology was observed (Fig. 2b). The UFT preparation was selected on the basis of its higher phenolic content (Table 1). Next, UVB dose was selected considering previous reports using the same irradiation unit on keratinocyte cell lines (23,24). In this study, a 25 mJ cm^{-2} UVB dose was enough to cause an approximate 26% decrease in NHEKs cell viability; as well as evident morphological changes consistent with cell death (Fig. 2a,b).

The UVB-induced decrease in cell viability was not prevented by either treatment with the UFT BBJ (Fig. 2a). However, as observed in the phase contrast microscopy, the UVB-mediated morphological damages were reduced in both 1:300 and 1:500 posttreatments (Fig. 2b). Consistently, there was also no antioxidant protective effect of the BBJ against UVB-induced total cellular oxidation; in fact, no significant antioxidant effect was observed at all for the UFT BBJ in this study (Fig. 2c). Nevertheless, the relatively high antioxidant capacity of *R. adenotrichos* fruit has been well established in previous studies using other systems for measuring antioxidant activity such as oxygen radical absorbance capacity and 2,2'-diphenyl-1-picrylhydrazyl free radical scavenging potential (16,26–28) and in a cellular antioxidant assay with erythrocytes (29). Azofeifa *et al.* (28) also showed that *R. adenotrichos* BBJ protected against lipid peroxidation in a liver model and in liposomes.

UFT BBJ protects NHEKs against UVB-mediated DNA oxidation and direct DNA damage

Photochemical damage to DNA is considered a critical factor in skin cancer development (30). UVB-mediated DNA damage occurs mainly in the form of CPDs and base oxidation by reactive oxygen species (31). Unrepaired CPDs might initiate photocarcinogenesis by causing UV-signature mutations in the form of C to T and CC to TT transitions (32,33), whereas guanine oxidation (in the form of 8-oxo-7,8-dihydro-2'-deoxyguanosine) can

generate G to T or A to C transversions (33). UVB-induced CPDs and 8-oxodG formation was confirmed in NHEKs and in SEs by immunochemistry (Figs. 3–5), indicating that the UVB 25 mJ cm⁻² dose was effective in causing potentially carcinogenic DNA damage.

Even though it was not possible to demonstrate if global cellular oxidation was affected by UFT BBJ, UVB-mediated oxidatively generated damage to DNA (in the form of 8-oxodG formation) was quenched by all UFT treatments, especially in the 1:500 posttreatment (Fig. 3), suggesting that BBJ could protect against photocarcinogenesis by reducing guanine oxidation. Furthermore, it is to be noticed that treatment with BBJ alone seems to have even reduced the naturally occurring base-line guanine oxidation observed in the untreated control (Fig. 3b), which might indicate relevant antioxidant properties for BBJ. However, further experimentation will have to be conducted for correlating the antioxidant properties of the BBJ with a direct photochemoprotective effect.

In accordance with previous reports, where treatment with other plant polyphenols has shown to be able to inhibit or repair UV-mediated DNA damage in skin cells, reconstituted SEs and animal models (reviewed in 5), UFT BBJ also reduced CPDs in both NHEKs (Fig. 4a) and SEs (Fig. 5b), supporting the evidence of chemoprotective properties of BBJ against UVB-induced DNA damage. Validation of the cell culture data in the 3D skin model also supports the possibility of a systemic effect. In addition, UVB-mediated activation of p53 by phosphorylation at serine 15 was also evidently reduced in the posttreatments (Fig. 4b). p53 is considered the “guardian of the genome,” inducing cell cycle arrest, DNA repair and apoptosis when DNA damage occurs (34,35). Its reduced activation in this study could suggest an indirect evidence of a general decrease in UVB-induced DNA damage by BBJ treatment. Together, these results indicate that systemic treatment with UFT was effective for reducing DNA damage in both UVB-irradiated NHEKs and SEs, potentially suppressing UV initiating carcinogenic stimuli.

UFT BBJ increased UVB-mediated apoptosis in NHEKs

UV-induced altered DNA photoproducts in the skin activate important signaling cascades, including apoptosis, cell cycle arrest and activation of DNA repair mechanisms; which, if impaired, can lead to carcinogenic mutations (5). Elimination of damaged cells by apoptosis is one of the primary defense responses of the epidermal cells against UV damage (36). PARP (116 kDa), a nuclear enzyme that functions as a facilitator for DNA repair, is inactivated after extensive DNA damage via effector caspases during apoptosis induction; hence, inactive cleaved PARP (~85 kDa) has been amply used a biomarker of apoptosis (37,38; reviewed in 39). In this study, detection of apoptotic cells by annexin staining showed that treating NHEKs with UFT BBJ before (2 h) or after (24 h) UVB irradiation (25 mJ cm⁻²) resulted in no observable changes in comparison to the irradiated control (Fig. 6a); however, immunoblot analysis evidenced a clear increase in PARP cleavage by both 1:500 UFT pre- and posttreatments, with a stronger effect in the pretreatment (Fig. 6b). As expected, PARP cleavage was evidenced in the UVB-irradiated cells, but not in the untreated control neither in cells treated with BBJ alone. These data suggest that UFT BBJ treatment enhanced only the UVB-mediated apoptotic response, which supports our hypothesis that BBJ might have a photochemoprotective effect by eliminating the UVB-damaged cells. Given that p53 activation was also reduced by the BBJ treatments, it is possible that the increased apoptotic response seen in this study might involve a p53-independent mechanism yet to be identified.

As mentioned above, *R. adenotrichos* has the highest content of ellagitannins ever reported in any other edible fruit (16,18). It has been shown that ellagic acid treatment induces apoptosis in a caspase-dependent pathway, with associated activation of PARP and caspases 3, 6, 8 and 9 (37). Thus, we studied caspases modulation next. Caspases are a family of

cysteine proteases, known for modulating cell death, inflammatory responses and differentiation by cleaving several target proteins. Caspase 8 is a transducer of the extrinsic apoptotic pathway, mainly via death receptor activation; whereas caspase 9 acts a downstream amplifier of the intrinsic mitochondrial apoptotic signaling. Caspases 8 and 9 are initiator caspases, performing signaling functions along the apoptosis cascade, whereas caspase 3 is one of the executioner caspases that directly activate the apoptosis effectors (reviewed in 38,40,41). In this study, both pre- and posttreatments with the 1:500 UFT dilution showed an enhanced activation of caspase 3 in comparison to the UVB irradiated cells, especially in the pretreatment (Fig. 7), supporting our previous PARP results and strongly suggesting that UFT BBJ treatment can, in fact, increase the UVB-mediated apoptotic response. As expected, UVB irradiation (25 mJ cm^{-2}) caused a strong apoptotic induction, evidenced by typical PARP cleavage and active caspase 3 expression. Treating NHEKs with UFT BBJ alone did not induce any observable apoptotic response, as confirmed by annexin staining and immunoblot analysis of PARP and caspases 3, 8 and 9.

In addition, both UFT BBJ dilutions (1:300 and 1:500) also increased caspase 8 cleavage; again, with a stronger effect in the pretreatment (Fig. 7). However, it was not possible to detect any observable caspase 9 cleaved products, which we believe was a defect in the antibody used for detecting this apoptotic marker. Nevertheless, caspase 9 proform expression is reduced in the UFT-treated samples, particularly those treated with the 1:300 dilution. These data indicate that the apoptotic response mediated by the UFT BBJ in the UVB-irradiated cells was activated through both the extrinsic and intrinsic pathway, suggesting a possible interaction with the membrane bound death receptors and possible mitochondrial failure. Thus, further studies will have to be conducted to elucidate possible death receptor activation by BBJ treatment, as well as its involvement in the intrinsic apoptotic response, and will be addressed in ongoing studies.

Taken together, our results indicate that systemic treatment with UFT BBJ was effective in reducing both CPDs and 8-oxodG in UVB-irradiated NHEKs, potentially suppressing the initiating carcinogenic stimuli, via increased apoptosis of the UVB-damaged cells. Here, we showed that UFT BBJ treatment enhanced apoptosis of cells that were damaged by UVB, potentially preventing carcinogenesis by stopping the progression of cells that might have genotoxic damage. However, PARP cleavage and caspases activation were clearly more intense in all pretreatments, suggesting that UFT BBJ could also predispose the cells to UVB-mediated apoptosis, a hypothesis for which further experimentation will need to be conducted. In addition, more studies need to be performed for discovering BBJ involvement in other cellular signaling responses, such as cell-cycle modulation and DNA repair mechanisms.

Acknowledgments

The authors thank M. Soto from CITA, and M.I. Chaves-Rodríguez from LAINTEC for their technical assistance. We also thank Instituto Tecnológico de Costa Rica (project 5401-1510-8901 and Programa de Becas), Universidad de Costa Rica (project 810-B2-231) and Fondo de Incentivos (CONICIT-MICIT, Costa Rica) for their financial support.

REFERENCES

1. Khan N, Syed DN, Pal HC, Mukhtar H, Afaq F. Pomegranate fruit extract inhibits UVB-induced inflammation and proliferation by modulating NF- κ B and MAPK signaling pathways in mouse skin. *Photochem. Photobiol.* 2012; 88:1126–1134. [PubMed: 22181855]
2. Boyle, P.; Levin, B. *World Cancer Report 2008*. Lyon, France: International Agency for Research on Cancer; 2008.

3. F'guyer S, Afaq F, Mukhtar H. Photochemoprevention of skin cancer by botanical agents. *Photodermatol. Photoimmunol. Photomed.* 2003; 19:56–72. [PubMed: 12945805]
4. Baliga MS, Katiyar SK. Chemoprevention of photo-carcinogenesis by selected dietary botanicals. *Photochem. Photobiol. Sci.* 2006; 5:243–253. [PubMed: 16465310]
5. Afaq F, Katiyar SK. Polyphenols: Skin photoprotection and inhibition of photocarcinogenesis. *Mini Rev. Med. Chem.* 2011; 11:1200–1215. [PubMed: 22070679]
6. Lomas A, Leonardi-Bee J, Bath-Hextal F. A systematic review of worldwide incidence of nonmelanoma skin cancer. *Br. J. Dermatol.* 2012; 166:1069–1080. [PubMed: 22251204]
7. Syed DN, Mukhtar H. Botanicals for the prevention and treatment of cutaneous melanoma. *Pigment Cell Melanoma Res.* 2011; 24:688–702. [PubMed: 21426532]
8. Katiyar S, Elmets CA, Katiyar SK. Green tea and skin cancer: Photoimmunology, angiogenesis and DNA repair. *J. Nutr. Biochem.* 2007; 18:287–296. [PubMed: 17049833]
9. Seeram NP. Berry fruits for cancer prevention: Current status and future prospects. *J. Agric. Food Chem.* 2008; 56:630–635. [PubMed: 18211019]
10. Boivin D, Blanchette M, Barrette S, Moghrabi A, Béliveau R. Inhibition of cancer cell proliferation and suppression of TNF-induced activation of NFκB by edible berry juice. *Anticancer Res.* 2007; 27:937–948. [PubMed: 17465224]
11. Duthie SJ. Berry phytochemicals, genomic stability and cancer: Evidence for chemoprotection at several stages in the carcinogenic process. *Mol. Nutr. Food Res.* 2007; 51:665–674. [PubMed: 17487926]
12. Stoner GD, Wang L-S, Casto BC. Laboratory and clinical studies of cancer chemoprevention by antioxidants in berries. *Carcinogenesis.* 2008; 29:1665–1674. [PubMed: 18544560]
13. González E, Vaillant F, Pérez A, Rojas G. *In vitro*-cell-mediated antioxidant protection of human erythrocytes by some common tropical fruits. *J. Nutr. Food Sci.* 2012; 2:139.
14. Huang WY, Zhang HC, Liu WX, Li CY. Survey of antioxidant capacity and phenolic composition of blueberry, blackberry, and strawberry in Nanjing. *J. Zhejiang Univ.-Sci. B (Biomed., Biotechnol.)* 2012; 13:94–102.
15. Lee J, Dossett M, Finn CE. *Rubus* fruit phenolic research: The good, the bad, and the confusing. *Food Chem.* 2012; 130:785–796.
16. Acosta-Montoya O, Vaillant F, Cozzano S, Mertz C, Pérez AM, Castro MV. Phenolic content and antioxidant capacity of tropical highland blackberry (*Rubus adenotrichus* Schldl.) during three edible maturity stages. *Food Chem.* 2010; 119:1497–1501.
17. Mertz C, Cheyner V, Günata Z, Brat P. Analysis of phenolic compounds in two blackberry species (*Rubus glaucus* and *Rubus adenotrichos*) by high-performance liquid chromatography with diode array detection and electrospray ion trap mass spectrometry. *J. Agric. Food Chem.* 2007; 55:8616–8624. [PubMed: 17896814]
18. Kaume L, Howard LR, Devareddy L. The blackberry fruit: A review on its composition and chemistry, metabolism and bioavailability, and health benefits. *J. Agric. Food Chem.* 2012; 60:5716–5727. [PubMed: 22082199]
19. Vaillant F, Pérez AM, Acosta O, Dornier M. Turbidity of pulpy fruit juice: A key factor for predicting cross-flow microfiltration performance. *J. Membr. Sci.* 2008; 325:404–412.
20. AOAC. Official Methods of Analysis of AOAC International. Gaithersburg, MD: AOAC International; 1999.
21. Chamcheu JC, Pihl-Lundin I, Mouyobo CE, Gester T, Virtanen M, Moustakas A, Navsaria H, Vahlquist A, Törmä H. Immortalized keratinocytes derived from patients with epidermolytic ichthyosis reproduce the disease phenotype: A useful *in vitro* model for testing new treatments. *Br. J. Dermatol.* 2011; 164:263–272. [PubMed: 20977447]
22. Chamcheu JC, Afaq F, Syed DN, Siddiqui IA, Adhami VM, Khan N, Singh S, Boylan BT, Wood GS, Mukhtar H. Delphinidin, a dietary antioxidant, induces human epidermal keratinocyte differentiation but not apoptosis: Studies in submerged and three-dimensional epidermal skin equivalent models. *Exp. Dermatol.* 2013; 22:342–348. [PubMed: 23614741]
23. Afaq F, Syed DN, Malik A, Hadi N, Sarfaraz S, Kweon M-H, Khan N, Zaid MA, Mukhtar H. Delphinidin, an anthocyanidin in pigmented fruits and vegetables, protects human HaCaT

- keratinocytes and mouse skin against UVB-mediated oxidative stress and apoptosis. *J. Invest. Dermatol.* 2007; 127:222–232. [PubMed: 16902416]
24. Syed DN, Afaq F, Mukhtar H. Differential activation of signaling pathways by UVA and UVB radiation in normal human epidermal keratinocytes. *Photochem. Photobiol.* 2012; 88:1184–1190. [PubMed: 22335604]
 25. Reyes-Carmona J, Yousef GG, Martínez-Peniche RA, Lila MA. Antioxidant capacity of fruit extracts of blackberry (*Rubus* sp.) produced in different climatic regions. *J. Food Sci.* 2005; 70:S496–S503.
 26. Mertz C, Gancel A-L, Gunata Z, Alter P, Dhuique-Mayer C, Vaillant F, Perez AM, Ruales J, Brat P. Phenolic compounds, carotenoids and antioxidant activity of three tropical fruits. *J. Food Comp. Anal.* 2009; 22:381–387.
 27. Gancel A-L, Feneuil A, Acosta O, Pérez AM, Vaillant F. Impact of industrial processing and storage on major polyphenols and the antioxidant capacity of tropical highland blackberry (*Rubus adenotrichus*). *Food Res. Int.* 2011; 44:2243–2251.
 28. Azofeifa G, Quesada S, Pérez AM. Effect of the microfiltration process on antioxidant activity and lipid peroxidation protection capacity of blackberry juice. *Rev. Bras. Farmacogn.* 2011; 21:829–834.
 29. González E, Vaillant F, Rojas G, Pérez AM. Novel semiautomated method for assessing *in vitro* cellular antioxidant activity using the light-scattering properties of human erythrocytes. *J. Agric. Food Chem.* 2010; 58:1455–1461. [PubMed: 20088504]
 30. Katiyar SK, Perez A, Mukhtar H. Green tea polyphenol treatment to human skin prevents formation of ultraviolet light B-induced pyrimidine dimers in DNA. *Clin. Cancer Res.* 2000; 6:3864–3869. [PubMed: 11051231]
 31. Yanagida J, Hammiller B, Al-Matouq J, Behrens M, Trempus CS, Repertinger SK, Hansen LA. Accelerated elimination of ultraviolet-induced DNA damage through apoptosis in CDC25A-deficient skin. *Carcinogenesis.* 2012; 33:1754–1761. [PubMed: 22764135]
 32. Afaq F, Adhami VM, Mukhtar H. Photochemoprevention of ultraviolet B signaling and photocarcinogenesis. *Mutat. Res.* 2005; 571:153–173. [PubMed: 15748645]
 33. Kappes UP, Luo D, Potter M, Schulmeister K, Rüniger TM. Short- and long-wave UV light (UVB and UVA) induce similar mutations in human skin cells. *J. Invest. Dermatol.* 2006; 126:667–675. [PubMed: 16374481]
 34. Li G, Ho VC, Mitchell DL, Trotter MJ, Tron VA. Differentiation-dependent p53 regulation of nucleotide excision repair in keratinocytes. *Am. J. Pathol.* 1997; 150:1457–1464. [PubMed: 9095000]
 35. Moll UM, Schramm LM. p53: An acrobat in tumorigenesis. *Crit. Rev. Oral Biol. Med.* 1998; 9:23–37. [PubMed: 9488246]
 36. Pradhan S, Kim HK, Thrash CJ, Cox MA, Mantena SK, Wu J-H, Athar M, Katiyar SK, Elmets CA, Timares L. A critical role for the proapoptotic protein bid in UV-induced immune suppression and cutaneous apoptosis. *J. Immunol.* 2008; 181:3077–3088. [PubMed: 18713978]
 37. Malik A, Afaq S, Shahid M, Akhtar K, Assiri A. Influence of ellagic acid on prostate cancer cell proliferation: A caspase dependent pathway. *Asian Pac. J. Trop. Med.* 2011; 4:550–555. [PubMed: 21803307]
 38. Degtarev A, Boyce M, Yuan J. A decade of caspases. *Oncogene.* 2003; 22:8543–8567. [PubMed: 14634618]
 39. Amé J-C, Spenlehauer C, de Murcia G. The PARP superfamily. *BioEssays.* 2004; 26:882–893. [PubMed: 15273990]
 40. Fuentes-Prior P, Salvesen GS. The protein structures that shape caspase activity, specificity, activation and inhibition. *Biochem. J.* 2004; 384:201–232. [PubMed: 15450003]
 41. Galluzzi L, Vitale I, Abrams JM, Alnemri ES, Baehrecke EH, Blagosklonny MV, Dawson TM, Dawson VL, El-Deiry WS, Fulda S, Gottlieb E, Green DR, Hengartner MO, Kepp O, Knight RA, Kumar S, Lipton SA, Lu X, Madeo F, Malorni W, Mehlen P, Nuñez G, Peter ME, Piacentini M, Rubinsztein DC, Shi Y, Simon HU, Vandenabeele P, White E, Yuan J, Zhitovitsky B, Melino G, Kroemer G. Molecular definitions of cell death subroutines: Recommendations of the

Nomenclature Committee on Cell Death 2012. *Cell Death Differ.* 2012; 19:107–120. [PubMed: 21760595]

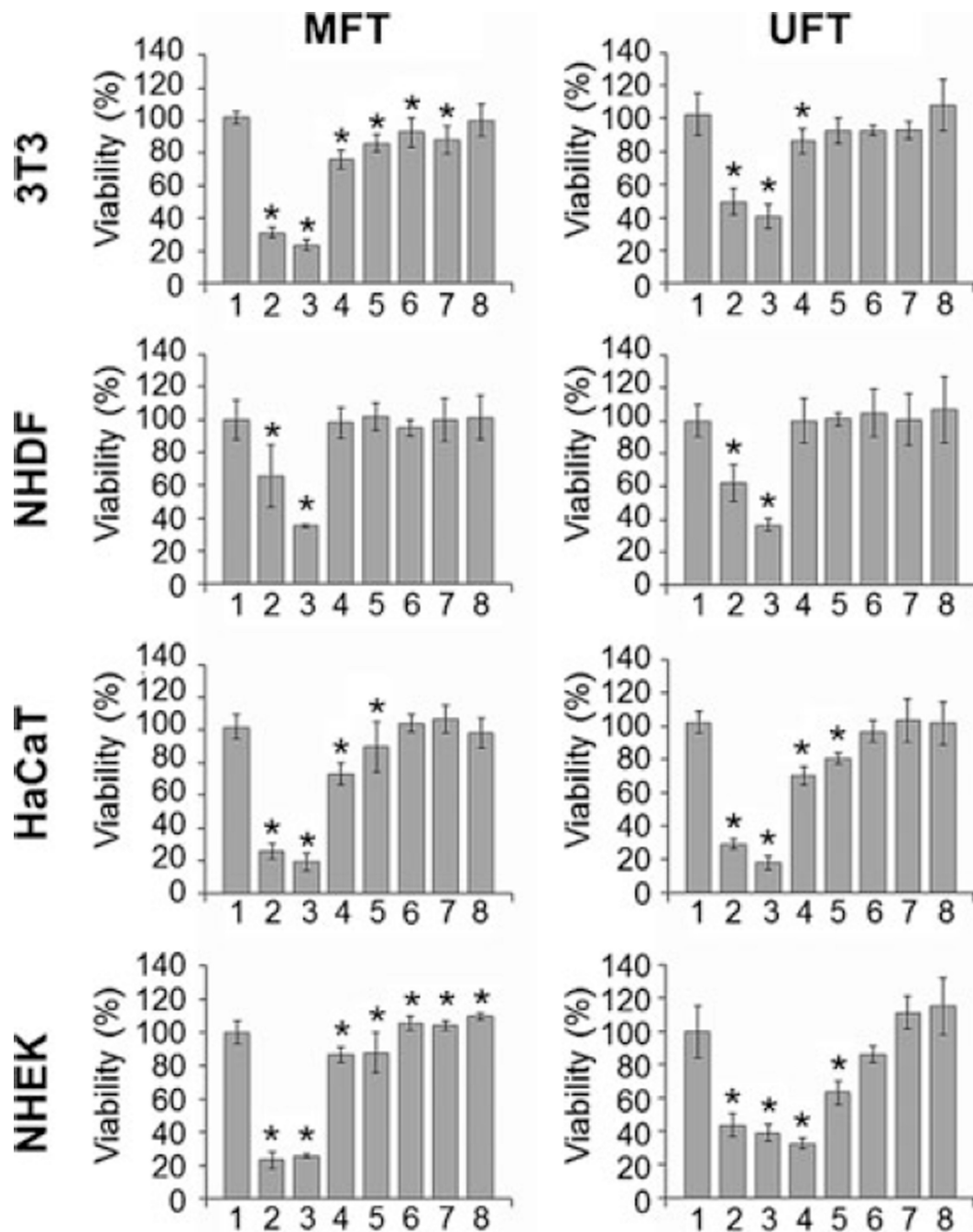


Figure 1.

Systemic application of blackberry juice (BBJ) has a similar effect on four different skin cell lines. Immortalized cell lines (3T3 and HaCaT) and normal cell lines (normal human dermal fibroblasts and normal human epidermal keratinocytes) were treated with different doses of microfiltered and ultrafiltered BBJ (1, untreated; 2, 1:5; 3, 1:10; 4, 1:50; 5, 1:100; 6, 1:150; 7, 1:300; 8, 1:500) for 24 h, after which cells were washed once with PBS and incubated for another 24 h in fresh media (to avoid bias by cytostatic effects) and harvested. Percent cell viability was assessed by MTT assay. Data shown represent the mean \pm SD of three

independent experiments in which each treatment was repeated in three wells. * $P < 0.05$ versus control.

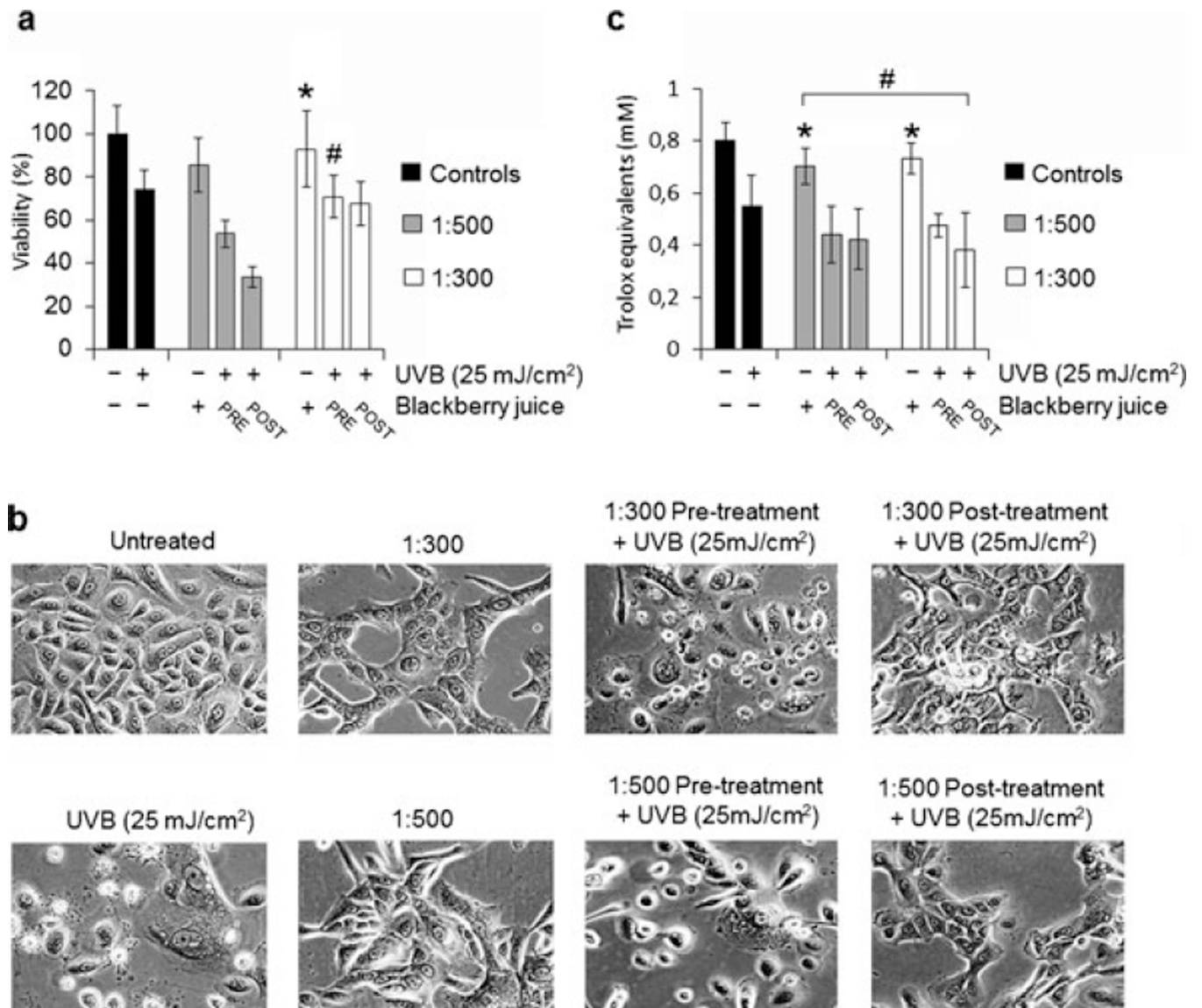
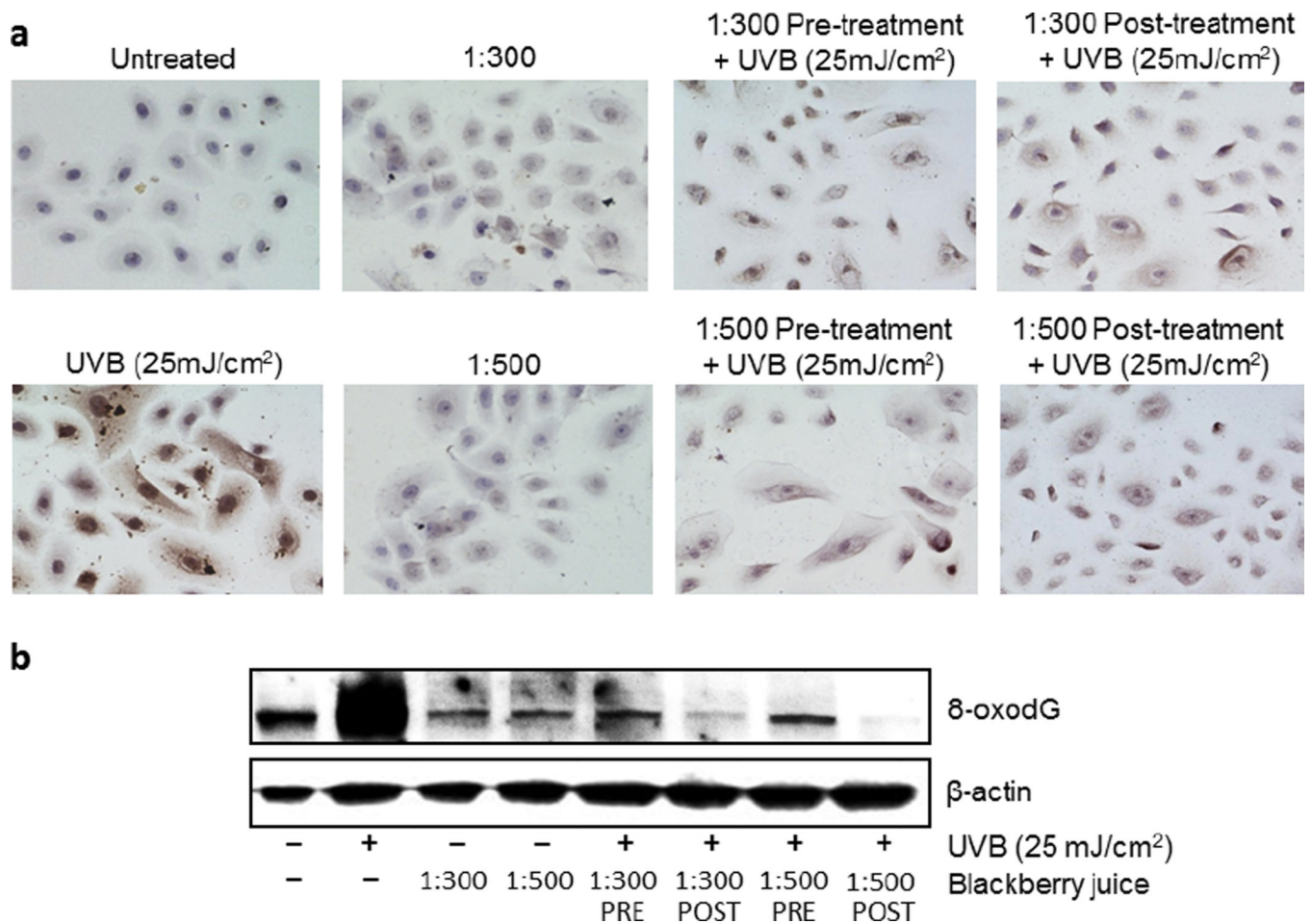


Figure 2. Ultrafiltered blackberry juice (UFT BBJ) does not protect normal human epidermal keratinocytes (NHEKs) against UVB-mediated decrease in cell viability and total cellular oxidation induced by UVB. NHEKs were treated with UFT BBJ for 2 h in the pretreatment and 24 h in the posttreatment, before or after exposure to UVB (25 mJ cm⁻²). Nonirradiated cells were treated with UFT BBJ for 24 h as controls. (a) Cells were harvested 24 h after UV irradiation, and percent cell viability was determined by MTT assay. (b) Phase contrast microscopy (10 ×) showing NHEKs treated with UFT BBJ before or after UVB irradiation (25 mJ cm⁻²). (c) Antioxidant activity was measured in NHEKs cell lysates by 2,2'-azino-di-[3-ethylbenzthiazoline sulfonate] oxidation assay as trolox equivalents. Data shown represent the mean ± SD of three independent experiments in which each treatment was repeated in three wells. **P* 0.05 versus untreated control, #*P* 0.05 versus UVB control.

**Figure 3.**

Ultrafiltered blackberry juice (UFT BBJ) protects normal human epidermal keratinocytes (NHEKs) against UVB-mediated DNA oxidation. NHEKs were pre- (2 h) and post (24 h) treated with UFT BBJ, before or after exposure to UVB (25 mJ cm⁻²). Nonirradiated cells were treated with UFT for 24 h as controls. (a) Twenty-four hours after treatment, NHEKs were processed by immunocytochemistry as described in “Materials and Methods,” and 8-oxo-7,8-dihydro-2'-deoxyguanosine (8-oxodG)-positive cells were detected as dark brown spotted cells ($n = 2$). (b) UVB-mediated 8-oxodG formation was determined by western blot. Equal loading was confirmed by reprobing the immunoblot for β -actin.

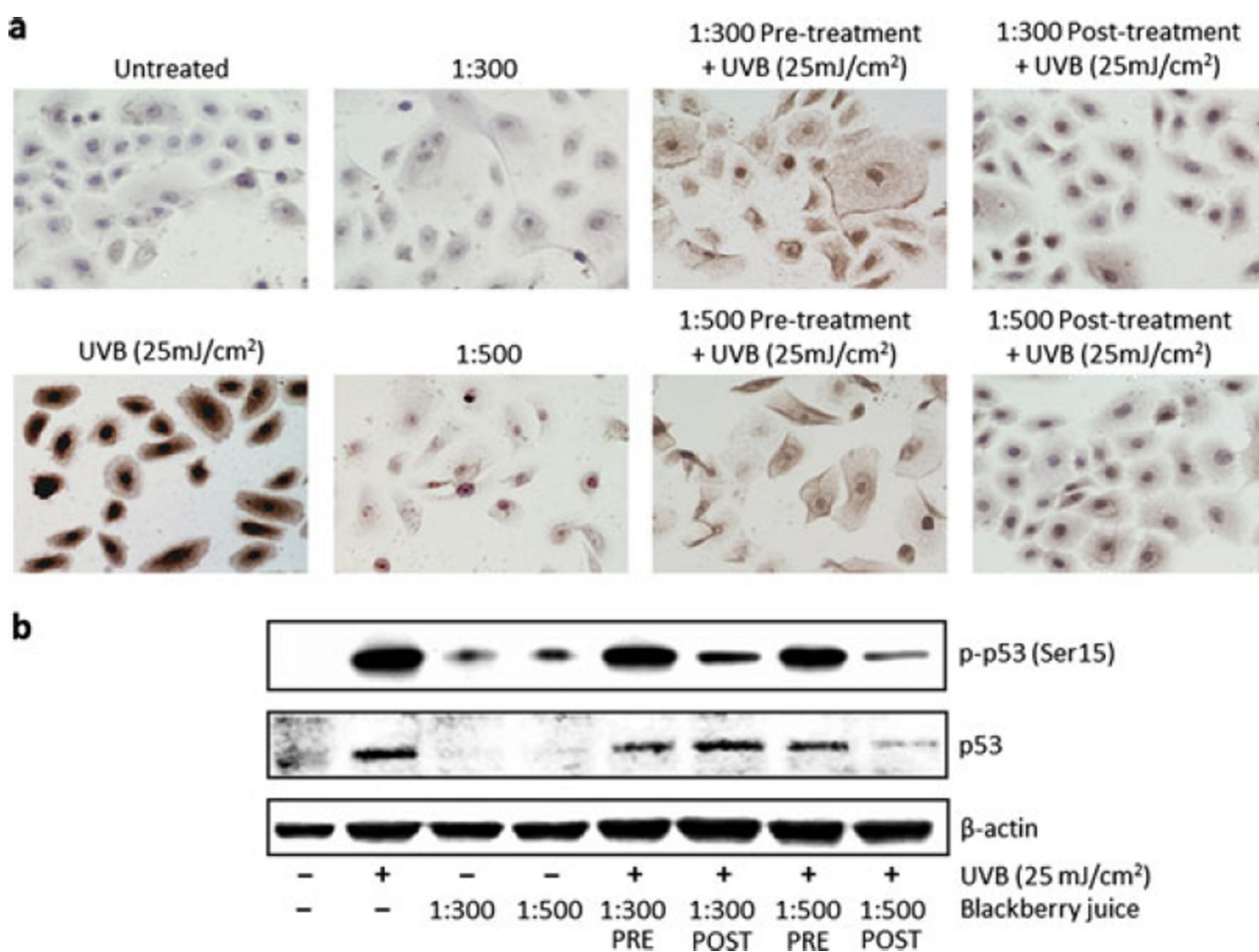


Figure 4.

Ultrafiltered blackberry juice (UFT BBJ) protects normal human epidermal keratinocytes (NHEKs) against UVB-mediated damage to DNA. NHEKs were treated with UFT BBJ for 2 h in the pretreatment and 24 h in the posttreatment before or after exposure to UVB (25 mJ cm⁻²). Twenty-four hours after treatment, cells were processed by immunocytochemistry (ICC) as described in “Materials and Methods,” or cell lysates were prepared for western blot analysis. (a) Cells were harvested 24 h after UVB irradiation, and cyclobutane pyrimidine dimer (CPD) ICC was performed as described in “Materials and Methods.” CPD-positive cells appear as dark brown cells in the samples ($n = 2$). (b) UVB-mediated p53 and p-p53 (Ser15) expression was determined by western blot. Equal loading was confirmed by reprobing the immunoblot for β -actin.

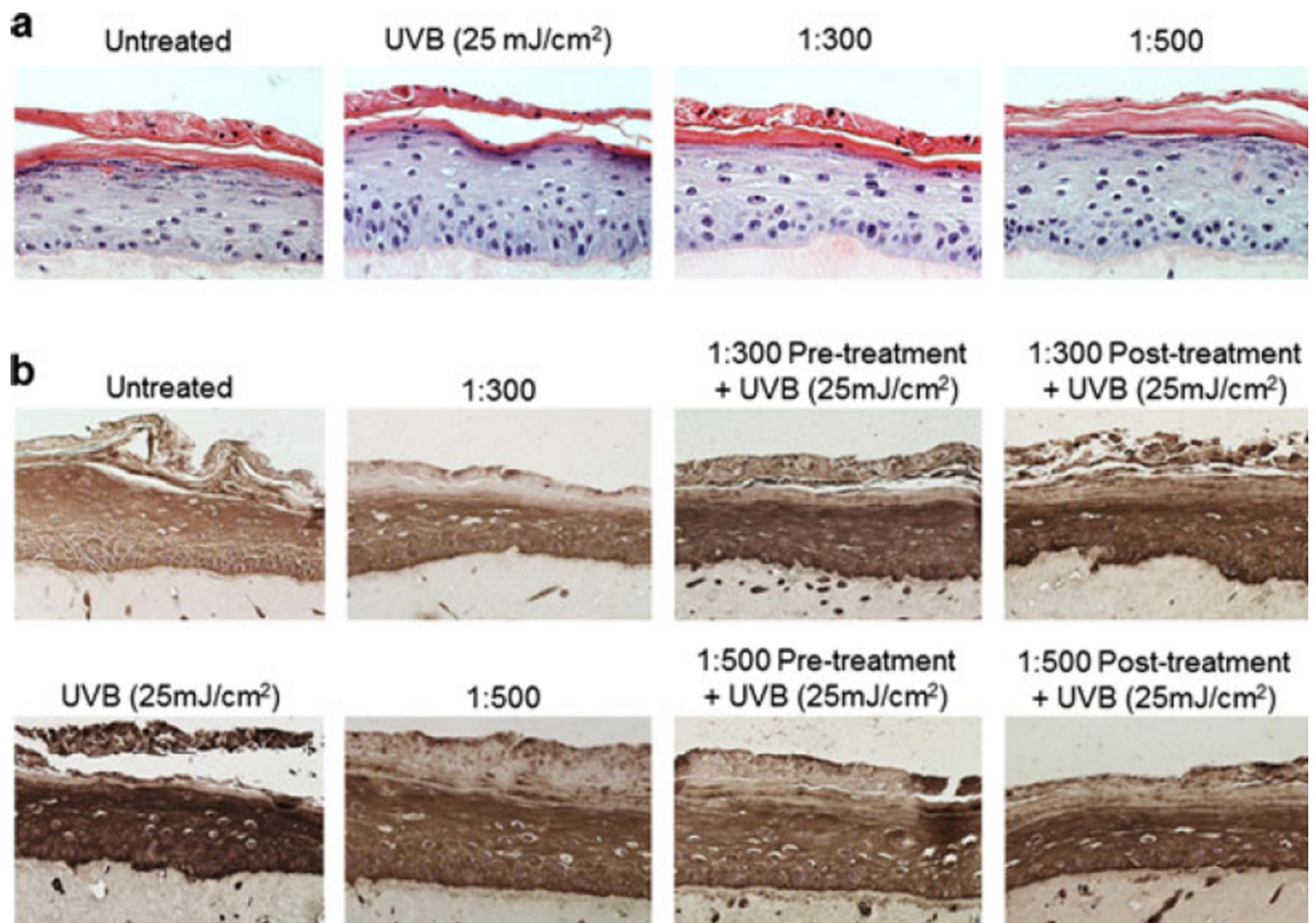


Figure 5.

Ultrafiltered blackberry juice (UFT BBJ) decreases UVB-induced cyclobutane pyrimidine dimers (CPDs) formation in SE. Three-dimensional reconstituted human skin equivalent was prepared as described in “Materials and Methods.” Tissue was treated with UFT BBJ for 2 h in the pretreatment and 24 h in the posttreatment before or after exposure to UVB (25 mJ cm⁻²). Nonirradiated tissue was treated with UFT for 24 h as controls. 24 h after treatment, formalin-fixed tissue was embedded in paraffin and processed by immunohistochemistry as described in “Materials and Methods.” (a) Representative hematoxylin and eosin–stained sections showed no relevant morphological difference between treatments ($n = 2$). (b) UVB-induced CPDs, seen as a dark brown immunostaining color, were reduced by all UFT treatments ($n = 2$).

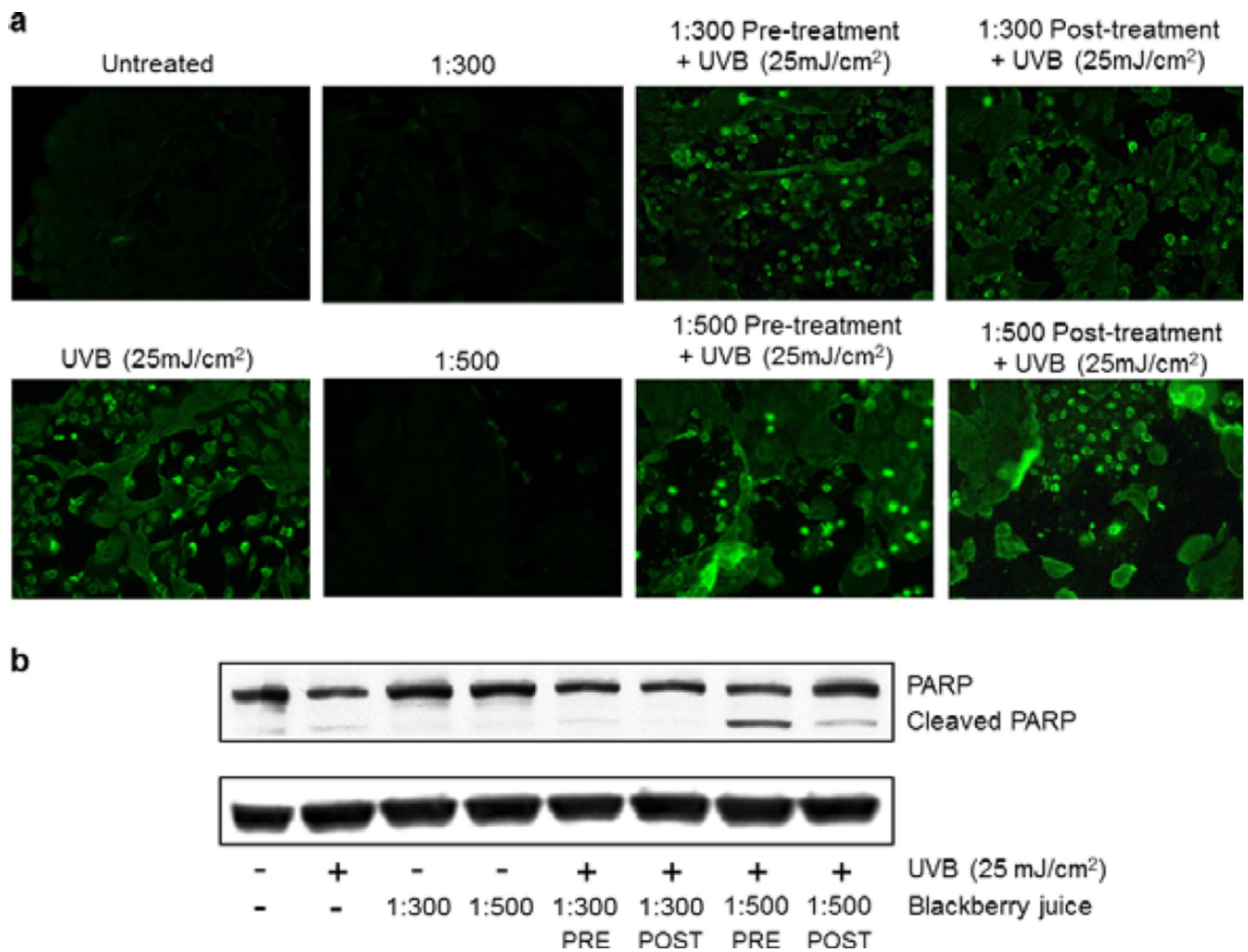


Figure 6.

Ultrafiltered blackberry juice (UFT BBJ) increased UVB-mediated apoptosis in normal human epidermal keratinocytes (NHEKs). NHEKs were pre- (2 h) and posttreated (24 h) with UFT blackberry juice before or after UVB irradiation (25 mJ cm⁻²) and harvested 24 h later. (a) UVB-mediated apoptosis (green) was detected by fluorescence microscopy using the annexin-V-FLUOS staining kit. Pictures shown are a representative of three independent experiments with similar results. (b) UVB-mediated poly(ADP-ribose) polymerase cleavage was determined by western blot. Equal loading was confirmed by reprobing the immunoblot for β -actin.

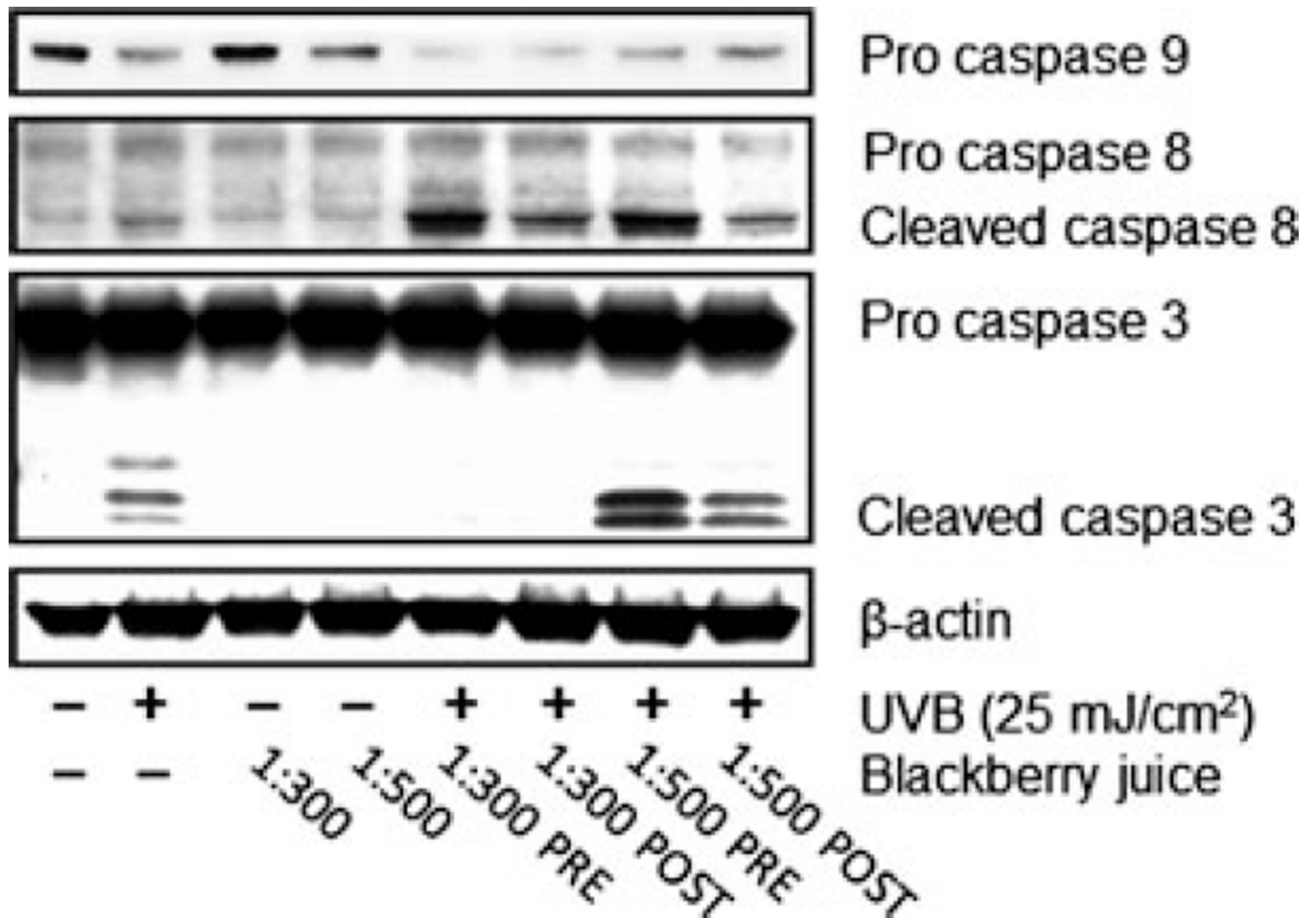


Figure 7. Ultrafiltered blackberry juice (UFT BBJ) modulates UVB-induced activation of caspases in normal human epidermal keratinocytes (NHEKs). NHEKs were pre- (2 h) and posttreated (24 h) with UFT BBJ before or after UVB irradiation (25 mJ cm^{-2}). Twenty-four hours later, cell lysates were prepared, from which protein expression was assessed by western blot. Equal loading was confirmed by reprobating the immunoblot for β -actin.

Table 1

Physicochemical properties of the blackberry juice (BBJ) used in this study.

Parameter	BBJ preparation	
	MFT	UFT
Soluble solids (°Brix)	10.2	11.3
Water content	88.9	88.6
pH	2.55	2.56
Total titratable acidity (g malic acid equivalents·100 g ⁻¹)	2.83	3.01
Ellagitannins (mg ellagic acid equivalents·L ⁻¹)	1418.95	2545.37
Anthocyanins (mg Cy-3-glc equivalents·L ⁻¹)	569.32	1016.46

MFT, microfiltered; UFT, ultrafiltered.